

## CLASSIFICATION OF SPECTROSCOPICAL IMAGERY BY COMBINING SPATIAL AND SPECTRAL INFORMATION: THE SSC METHOD

Tom HORNSTRA \*, Hans-Gerd MAAS\*, Steven DE JONG\*\*

\*Delft University of Technology, The Netherlands  
Faculty of Civil Engineering and Geo-Information

[t.j.hornstra@geo.tudelft.nl](mailto:t.j.hornstra@geo.tudelft.nl)

[h.-g.maas@geo.tudelft.nl](mailto:h.-g.maas@geo.tudelft.nl)

\*\*Wageningen University and Research Centre  
Centre for Geo-Information

[steven.dejong@staff.girs.wag-ur.nl](mailto:steven.dejong@staff.girs.wag-ur.nl)

Working Group VII/4

**KEY WORDS:** Hyperspectral, Classification, Image processing, Segmentation

### ABSTRACT

Classification of remotely sensed images is often based on assigning classes on a 'per-pixel' basis and therefore ignoring spatial information captured by the image. In this paper a method is proposed that combines spatial and spectral information in two steps. Spatial information is first extracted by segmentation: spectral homogeneous regions in the image are identified on the basis of similarity of the entire spectral shape from visible to shortwave infrared. These homogeneous areas are classified and next, this information is used to classify the remaining heterogeneous pixels. The method is applied and validated on DAIS images acquired over an area covered with natural vegetation and agricultural activities in southern France. Results indicate significant improvements of classification results compared to traditional per-pixel classifiers.

### 1 INTRODUCTION

Classification of remotely sensed images is one of the most widely used image interpretation methods in the remote sensing nowadays. The classification process is a (semi-)automatic way of image interpretation, where every pixel of the image is assigned to a by the analyst predefined class of group. These classes can be land cover classes such as soil or vegetation but also sources of environmental pollution or atmospheric hazards like tornados. Classified images are often used as input for information systems such as Geographical Information Systems or other analysis tools for geographical data and/or decision-making purposes (Burrough & MacDonnell, 1998).

The traditional approach of classifying remotely sensed images is to compare the characteristics of each pixel with predefined classes and assign a label to the the pixel on the basis of solely their spectral characteristics and on statistical characteristics of the classes (e.g. the maximum likelihood classification). This approach has widely been used for the analysis of all kinds of remotely sensed images, with varying succes. In last the decennium, the spectral as well as the spatial resolution of the remote sensing sensors has dramatically improved. This increase of Spatial and Spectral information enables us to apply more deterministic approaches to the classification process than only making statistical assumptions.

Imaging spectroscopy (or hyperspectral remote sensing) sensors record a large part of the EM spectrum simultaneously in a large number of small bands, providing us a contiguous part of the EM spectrum with unique absorption features (Goetz et al., 1985). Using this technique it is possible to create a spectral profile plot, or a spectral signature for each pixel and for every class in the image. Techniques have been developed to use this additional information for improving the classification of spectroscopical images such as cross correlogram spectral matching (Van der Meer & Bakker 1997), spectral angle mapper (Kruse *et al.* 1993) and the tricorder algorithm (Crósta *et al.* 1996).

The main disadvantage of the traditional methods is that the spatial component in the image is ignored. A remotely sensed image is a representation of the earth surface and therefore a pixel does have a relation with its neighbouring pixels and most probably also with pixel at a larger distance. Various studies have shown that it is possible to include spatial information in the classification process by describing the texture in an image and by using the textural information to enhance the classification results, methods such as combination of spectral and texture data (Ryherd &

Woodcock 1996), semi-variograms (St-Onge 1999, De Jong & Burrough 1995) and intra-pixel reflectance variability (Hornstra *et al.* 1999). Although it was shown that these methods are capable of improving the results of a classification, the use of textural information is still an indirect way of including spatial information.

Another method to include spatial information in the classification process is the use of additional geographical information such as vector data. It is possible to classify the remote sensing images per field rather than per pixel. Results from these approaches show great improvements in classification results (Jansen & Molenaar 1995, Aplin *et al.* 1999). However, these methods require additional data sources and cumbersome data integration steps. Other methods include segmentation of the image into regions of interest before a classification (Kettig & Landgrebe 1976, Bryant 1979, McCormick 1996).

In this study a theoretically similar method is proposed. This new method takes the spatial as well as the spectral increase of information into account for improving the image classification. The procedure has been implemented and tested on spectroscopical images acquired by the DAIS sensor having a high Spatial and Spectral resolution. In this paper the new proposed method is discussed and applied to DAIS imagery. The method is validated using images and a field data set from a test area in southern France.

## 2 COMBINATION OF SPATIAL AND SPECTRAL DATA IN THE CLASSIFICATION PROCESS

### 2.1 The Spatial and Spectral Classification (SSC) method

Since a remotely sensed image is a spatial representation of the surface of the earth, spatial information is believed to be a valuable information source in the classification process. One possible element of spatial information in a remotely sensed image is a homogeneous region. A homogeneous region in the remote sensing image is often a field or another area of interest in the map if that is the result of the classification. Therefore the goal of this research was to extract information from homogeneous regions in a remotely sensed image to use in the classification process. This is realised in the Spatial and Spectral classification method (SSC). The SSC method is conducted in two steps, that can be discriminated as the coarse and the fine step. In the first (coarse) step the location of the homogeneous regions is

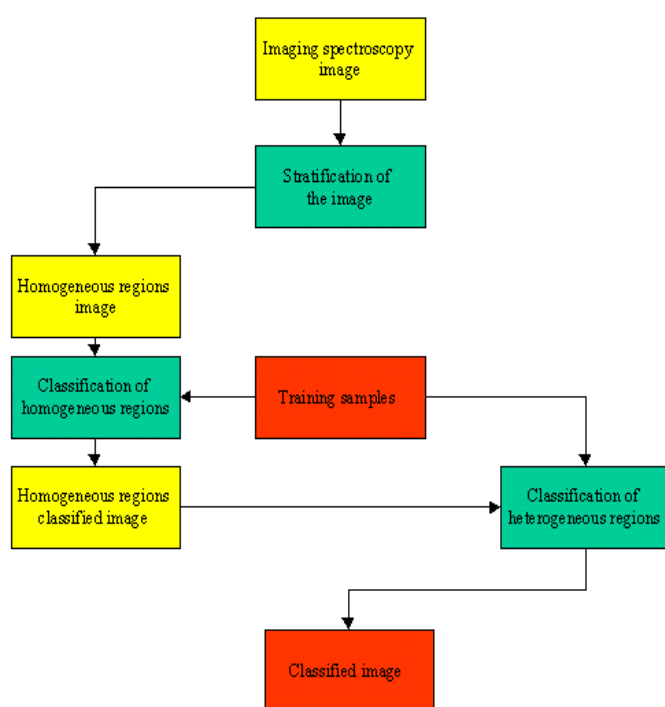


Figure 1. Scheme of the Spatial and Spectral Classification (SSC) method. The image is divided in homogeneous regions and heterogeneous regions. After classification of homogeneous regions this additional information is applied for classifying the remaining regions.

extracted from the image by segmentation of the image. In the next step the homogeneous regions are extended by using a combination of spectral information from the pixels and spatial information based on the position of the homogeneous regions. Therefore this last step can be considered as the fine-tuning step.

In the fine-tuning of the classification process, the spatial information should contribute to the assigning of the remainder of the pixels to a class. Basic assumption is that pixels are spatially correlated, but all kinds of errors like mixing of classes in one pixel, sensor noise or atmospheric disturbances prevent the pixels being classified to the same class. For those reasons it is interesting to determine if the pixel is likely to belong to the same homogeneous region or to the same class in the classified image. In order to achieve this information homogeneous areas have to be classified, so that information on the location of classes is available. In the SSC method the following three steps can be discriminated (as shown in figure 1):

- 1) Spatial and Spectral Extraction of homogeneous regions
- 2) Classification of the homogeneous regions
- 3) Classification of the remaining areas

These steps are described in detail in the next sections.

## 2.2 Stratification of the image

The objective of the *stratification stage* is to identify homogeneous regions in the remote sensing image. Imaging spectroscopy sensors are able to create a contiguous representation of the reflectance of EM solar radiation on a pixel-per-pixel basis, which can be visualized using the spectral profile plot. In this research the spectral profile plot is used to compare pixels with one another in a neighbourhood system for determining their similarity. Therefore first a neighbourhood system is defined which in this case is the 4 neighbourhood system  $N$ .  $N$  includes the center pixel and its four direct neighbours (left, right, under, above) and can be defined by:

$$N_i = \{j \mid \|i - j\| = 1\} \quad (1)$$

where  $i$  are the co-ordinates of pixel  $i$ ,  $N_i$  is the defined neighbourhood system for pixel  $i$  and  $j$  are the co-ordinates of a pixel included in  $N$ . To determine whether the pixels in the neighbourhood system are similar to a certain degree, the spectral profile plot of all pixels in  $N$  are compared with the center pixel by using a relative bandwidth for the spectral signature of pixel  $i$ . If the spectral signatures of all the pixels in  $N$  lie within this bandwidth,  $N$  is considered to be homogeneous:

$$T \geq \left\{ \begin{matrix} n \\ p=1 \end{matrix} \left| x_{ip} - x_{jp} \right| \forall j \in N_i \right\} \quad (2)$$

where  $T$  is a predefined threshold value, that describes a measure of similarity between pixel  $i$  and pixel  $j$  within  $N$ ,  $n$  is the number of spectral bands within the image,  $x_{ip}$  is the reflectance value for pixel  $i$  in band  $p$  and  $x_{jp}$  is the reflectance value for pixel  $j$  in band  $p$  within  $N$ .

The result of the stratification stage is a division of the image into homogeneous and heterogeneous regions. A homogeneous region in the image comprise at least 5 pixels, as this is the minimum number in the defined neighbourhood system. However, a homogeneous region can consist of various adjacent neighbourhood systems and therefore a homogeneous region is usually larger than 5 pixels.

## 2.3 Classification of the homogeneous areas

The result of the stratification stage is a division of the image into homogeneous regions and heterogeneous regions. In this stage the homogeneous regions of the image are classified. Therefore every homogeneous region ( $H$ ) in the image is assigned with a unique number. This number serves as identification for the homogeneous regions in the image. Next, the general spectral signature of every homogeneous region  $H$  is calculated by assigning to every pixel in  $H$  the averaged reflectance value of  $H$ , or:

$$\bar{x}_{ip} = \left\{ \begin{matrix} m \\ q=1 \end{matrix} \frac{x_{ip}}{m} \mid \forall i \in H_i \right\} \quad (3)$$

where  $\bar{x}_{ip}$  is the averaged value for pixel  $i$  in band  $p$ ,  $H_i$  is the homogeneous area that includes pixel  $i$  and  $m$  is the number of pixels within  $H_i$ . In this way the general spectral signature can be calculated for every pixel in a homogeneous region and that can be done for all homogeneous regions.

At this point training samples are collected for the classification of the homogeneous regions (figure 1). Based on these training samples the homogeneous regions are classified using the Minimum Distance To Mean (MDTM) classifier. Because all pixels in a homogeneous region carry the same average value, all pixels in one homogeneous area are classified into the same class by definition of the classifier. A mask is used to exclude heterogeneous areas from this classification step. The here proposed method has now yielded an intermediate result where homogeneous areas are classified and heterogeneous pixels are not yet considered.

## 2.4 Classification of the heterogeneous areas

The classification of the heterogeneous pixels is the next step in the classification process. In this stage the remaining unclassified pixels in the image are classified by using both Spatial and Spectral information. Therefore the MDTM classifier is adapted to use both Spatial and Spectral information. A normal MDTM classification consists of the calculation of the Euclidean spectral distance in the feature space between the mean of every class and the pixel to be classified. The distance between the mean of a class and a pixel in the feature space is calculated by:

$$d_{\omega}^{spec} = \|i - z_{\omega}\| \quad (4)$$

where  $d_{\omega i}^{spec}$  is the spectral distance between the co-ordinates of pixel  $i$  and  $z_{\omega}$ , the co-ordinates center of the training samples of class  $\omega$ . The pixel is then assigned to the class  $\omega^*$  where  $d_{\omega i}^{spec}$  is minimal:

$$\omega^* = \min_{\omega} d_{\omega i}^{spec} \quad (5)$$

To account for the spatial information in the procedure, equation (5) is extended by introducing the spatial distance  $d_{\omega i}^{spat}$ :

$$\omega^* = \min_{\omega} (\alpha \times d_{\omega i}^{spec} + (1 - \alpha) \times d_{\omega i}^{spat}) \quad (6)$$

where  $\alpha$  is a ratio factor for describing the influence between the spatial and the spectral part and  $d_{\omega i}^{spat}$  is a measure to describe the spatial distance of an unclassified pixel into a homogeneous classified region. The spatial distance  $d_{\omega i}^{spat}$  is calculated by defining a growing ring of pixels surrounding the unclassified pixel  $i$ . In the first run this ring exists of the 8 pixels that directly surround the pixel  $i$ , in the second run the ring exist of the 16 pixels that are surrounding the first ring and so on. Within every ring, the number of previously classified pixels is counted for every class. This number of classified pixels,  $\lambda_{\omega}$ , is then multiplied by a weightfactor as in (7):

$$d_{\omega i}^{spat} = \frac{\tau}{\Omega} \frac{1}{\lambda_{\omega} \times \prod_{\omega=1}^{\Omega} d_{\omega i}^{spec}} \quad (7)$$

where  $d_{\omega i}^{spat}$  is the inversed spatial distance from pixel  $i$  to the classified pixels for every class  $\omega$ , (the pixel is assigned to the class where the distance is *minimal* similar to the MDTM approach).  $\lambda_{\omega}$  is the total number of appearance of class  $\omega$  in the ring kernel,  $\tau$  is the total number of pixels in the ring kernel and  $\Omega$  is the total number of classes appearing in the image. To be sure that the influence of the spatial and the spectral part of the classifier are equal to eachother without the influence of the ratio factor  $\alpha$  in (6), the total sum of spectral distances is used as a weightfactor in (7). In case of maximum spatial and spectral influence for one class  $\omega$  these two are equal to each other:

$$\prod_{\omega=1}^{\Omega} d_{\omega i}^{spec} = \prod_{\omega=1}^{\Omega} d_{\omega i}^{spat} \quad (8)$$

The ratio factor  $\alpha$  in (6) is defining the influence between the spectral and spatial information. In case of an equal influence, the factor is set at 0.5. If the spatial influence  $\alpha$  is set at 0, it means that the remaining pixels are classified solely on their spectral characteristics as in the usual MDTM classification. If  $\alpha$  is set to 1, the pixels are classified using only spatial information, similar to a reclassification method, as for example in Bryant (1979).

The number of runs for the growth of the kernel ring is theoretically unlimited, but since the spatial information used is based on homogeneous regions in the image, it should only be used to enhance the edges of the homogeneous regions and unclassified pixels within the homogeneous regions. Although it is very likely that an unclassified pixel adjacent to a classified pixel can belong to the same class, this assumption can only be true for a limited number of pixels. Therefore it is suggested that only a small number of runs to extend the ring kernel is used e.g. in this research only two runs were used. We felt that for the test area a distance of two pixels was the maximum distance of spatial dependency. The pixels that were unclassified after two runs, were classified by using the normal MDTM classification.

### 3 TEST AREA AND PREPARATION OF THE DATASET

#### 3.1 Test area and the scanner data

The Digital Airborne Imaging Spectrometer DAIS 7915 was built by the Geophysical Environmental Research corp. (GER), funded by the the European Union and DLR (Deutsches Zentrum für Luft- und Raumfahrt). The sensor covers a spectral range from the visible to the thermal infrared wavelenghts at variable spatial resolution from 3 to 20 meters depending on the aircraft altitude. The DAIS 7915 is used since spring 1995 for remote sensing applications such as environmental monitoring of land and marine ecosystems, vegetation status and stress investigations, agriculture and forestry resource mapping, geological mapping, mineral exploration as well as for the supply of data for geographic information systems. More information on the DAIS 7915 scanner can be found on the website of Institut für Optoelektronik (2000).

In 1997 and 1998 the DAIS 7915 scanner has been used as part of the EU DEMON project to assess its usefulness for an interdisciplinary approach to land degradation such as desertification in the Payne catchment. The Payne catchment

is located in the South East of France between Montpellier and Béziers. More information on the DEMON project can be found on DeMon-II (2000). The first experimental flight was on the 8<sup>th</sup> of July 1997 under almost perfect conditions. Weather conditions were less during the second flight on the 28<sup>th</sup> of June 1998. Details on the performance of the scanner are described by De Jong *et al.* (1998). The flight altitude was in both cases 3000 meter, resulting in a ground resolution of 6 meter per pixel. During the second flight campaign in 1998 ground truth information was collected on the ground by surveying parcels using DGPS.

### 3.2 Preparation of the dataset and ground truth information

Because of the good quality of the first dataset collected in 1997, this data has been used during the comparative classification tests. Preprocessing of the data was necessary to acquire reflectance values and was done using an empirical line method and spectra collected in the field (De Jong *et al.* 1998). The image was stretched using a linear stretching technique and converted into a 8-bit datatype. To prevent mixing of pixel values as a result of a geometrical conversion, it was decided to reverse the normal geometrical correction process. In this case the ground truth dataset was geometrical corrected back into the local co-ordinate system of the flight image. 100 re-sampled points in the ground truth data and the image were collected and the ground truth data set was geometrically transformed into the image co-ordinate system using a rubber sheeting method in the GIS package ARC/INFO. Although the re-sampled points were collected with great care, the internal error of 12 meters forced to reduce the ground truth dataset with 2 pixels, which had the result that all reference data were located in the center of the agricultural lots or vegetation units. Since the ground truth dataset was collected in 1998, one year after the data acquisition date, all ground truth samples have been visually verified on the right class.

## 4 RESULTS OF THE COMPARATIVE TESTS AND DISCUSSION

Two test areas, simply called *North* and *South*, have been selected and extracted from the original image. The Spatial and Spectral Classification (SSC) method as described previously was implemented in IDL/ENVI remote sensing image visualising software. Classification of the test area has been carried out using the SSC method and conventional classification methods, and these were compared with one another by visual interpretation and by comparing the classified image with the ground truth dataset.

### 4.1 Results of the *South* test area

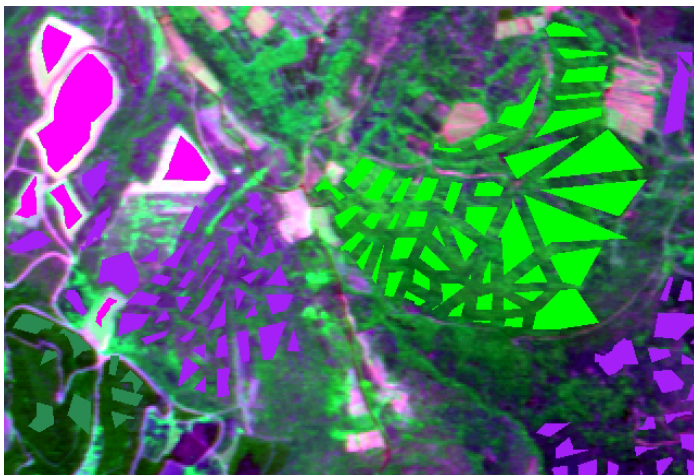


Figure 2. South test area (visualisation VIS-NIR-SWIR) in where ground truth areas are displayed. The ground truth areas have been surveyed in the field using DGPS and therefore cover large areas.

In the South test area (covering 1920 x 1296 meter), 4 classes were selected to represent the image, which are vineyards, maquis, garrigue and conifers. For all of these classes ground truth information was available. Ground truth was acquired in the field and therefore available in large surveyed areas as can be seen in figure 2.

For every class about 30% of the ground truth information was used as training samples. The remaining 70% of the ground truth information was used for validation of the classification and to make an assessment of the accuracy of the different classification techniques. The image stratification was carried out using a threshold value of 165 (eq.2), resulting in a bandwidth of 0.91%. Trial and error and a visual interpretation of the results gained this result. SSC

classification was carried out using a different impact ratio between the Spatial and Spectral information. Overall accuracy of the classification compared with ground truth raised with for about 8% in comparison with the best performing conventional classifier, Mahalanobis distance classification, as can be found in table 1:

Classifier	MDTM	Max. Lik.	Mahal. Dist.	SAM	SSC (50 %)	SSC (60%)	SSC (70%)
Overall Accuracy	83.64 %	80.14 %	84.09 %	68.11 %	92.45 %	92.66 %	92.73 %

Table 1: Confusion matrix overall accuracy results per classification method. All performances of the Spatial and Spectral Classifier (SSC) gain better results, mutual differences are small.

Visual interpretation between classified images reveals various differences between the classification methods. Figure 3, showing the classified images illustrates that the image classified with the SSC method, contains better defined homogeneous areas. Single lost pixels are only sparsely present. The maquis area in the SSC classified image is much larger. The usual spectral confusion in per pixel classifiers between classes is here avoided by defining the homogeneous region that are then classified at once.

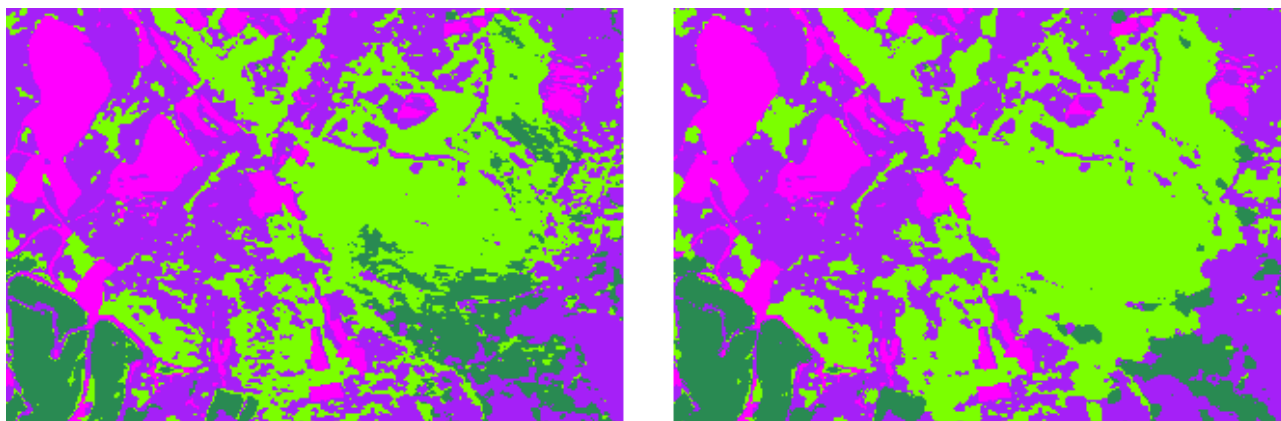


Figure 3. The image left is the result of the the MDTM classifier, the right image is the result of SSC classification, using a spatial impact ratio of 70% to classify the heterogeneous pixels. In the image right, regions are much more homogeneous and borders are better defined.

It is likely that the major improvement of the overall accuracy between the conventional classifiers and the SSC method is the result of the first classification step: the per-region classification. Due to the spatial coarseness of the ground truth dataset, it is difficult to determine the effect of the classification of the heterogeneous pixels on the final classification result. Changes in this part of the classification are mainly expected at the edges of homogeneous regions. Visual interpretation however, reveals the differences between the conventional and SSC classification method as shown in figure 4.

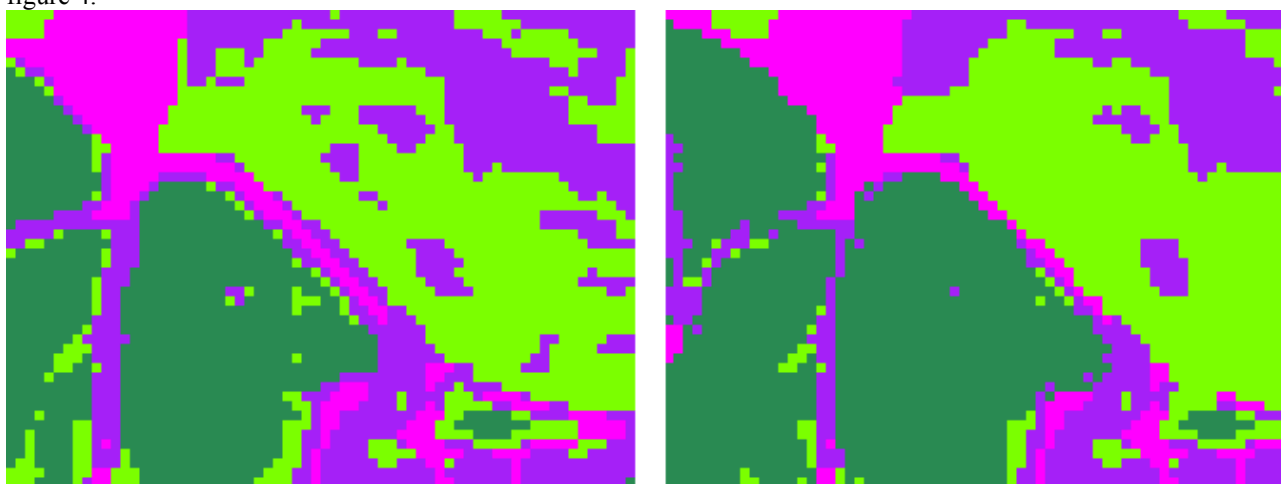


Figure 4. Magnification of a part of the classified images. The left image is classified using the MDTM classification method, the image on the right using SSC classification. Note the impact of the approach on the road in the center of the image.

In figure 4 the spatial impact of the SSC classifier becomes visible. In the left image, classified by the MDTM classification, a common problem of a per pixel classifier is visible: a salt and pepper pattern. And at the border of classes, mixed pixels occur. In a per pixel classification, these pixels are often labeled as 'unknown' due to the mixed spectral signature of the pixel. This can be seen in the image on the left. The small road is classified as 'vineyard', as

their spectral signature resembles. The adjacent pixels are not assigned to the class 'conifer' (dark green) nor to 'maquis' (green), which are adjacent classes. Instead they are classified as garrigue (purple). The new proposed method, using spatial information during the image classification, various of these mixed pixels are assigned to the correct class as shown in the image on the right.. An other indication for the better performance of the SSC methods is the road. The road is narrower in the right image, during the stratification approach the road is labeled as a heterogeneous area and as such its mixed spectral signature has a smaller impact during the classification stage of the SSC method.

#### 4.2 Results of the *North* test area

In the North test area only 3 ground truth classes were present in the image. It is apparent from figure 5 that these three classes are not sufficient to give an accurate classified representation of the area. Therefore, 5 land cover classes were selected being vineyards, bare soil, grassland, maquis and mining area. Ground truth was acquired likewise the method for the south test area.

Classifier	MDTM	Max. Lik.	Mahal. Dist.	SAM	SSC (50 %)	SSC (60%)	SSC (70%)
Overall Accuracy	88.67%	48.26%	61.41 %	69.04 %	92.04%	91.98%	91.84%

Table 2: Confusion matrix overall accuracy results per classification method. All performances of the Spatial and Spectral Classifier (SSC) gain better results, again mutual differences by spatial influence are small.

The same method was used in the classification of the North test area. One difference was that only three classes could be used for validation.. Stratification was carried out using a bandwidth of 0.96%. By calculating the confusion matrix the overall accuracy of the classification with three ground truth classes was computed. These results show an improvement for SSC classification. The SSC method produces a more homogeneous classified image as shown in figure 5. Figure 5 displays the classified images of the North test area for the MDTM classification (left) and the SSC classification with 70% spatial influence (right). The salt and pepper pattern is pre-dominantly present in the MDTM result compared to the SSC image.

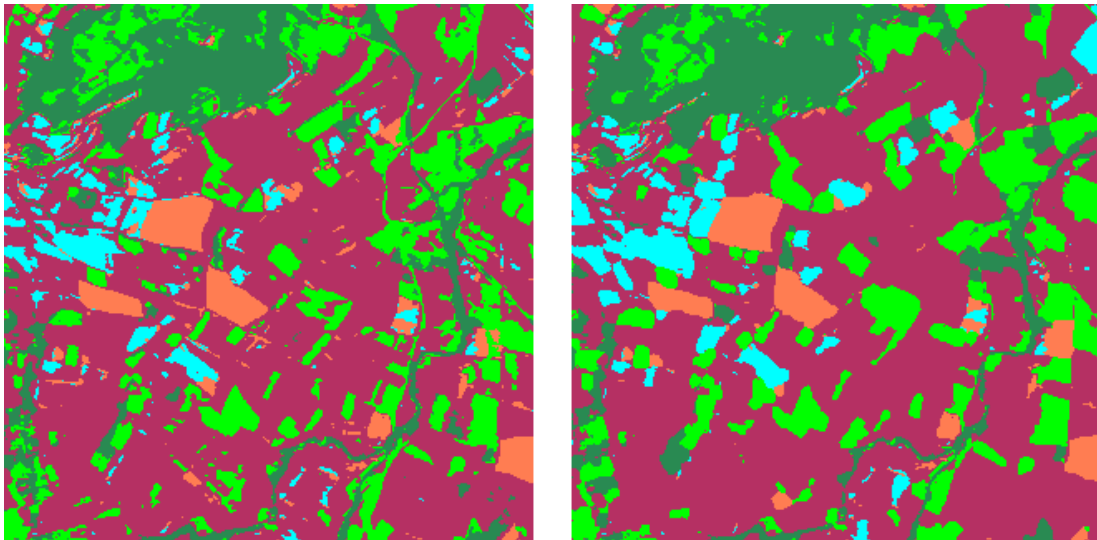


Figure 5. Classification results of the MDTM classification left and the SSC classification with 70% spatial influence on the right. Homogeneous regions in the right image are better defined.

#### 4.3 Discussion

The aim of producing the SSC classification method was to account for spatial information during the classification process. This was achieved in two steps First, homogeneous regions in the image were extracted and classified using a per-region classification. Next, the heterogeneous pixels ignored during the first step, are classified by combining Spatial and Spectral information in an adjusted MDTM classification. It is obvious that the regions extracted during the stratification mainly represent the center of a homogeneous area in the remote sensing image. Due to the presence of the ground truth data set in the center of homogeneous regions, and the absence at the borders, the results as mentioned above are most likely the result of the classification of the homogeneous regions. Therefore it is difficult to verify the 'fine tuning' of the classification, the second part of the SSC. Visual interpretation of the classified image showed that changing the spatial impact ratio in the final step of the classification can avoid problems encountered by per pixel classifiers.

Unlike the per pixel classifiers, the SSC method allows the user to interact with the classification process. The SSC method allows the extraction of homogeneous regions. In an iterative process, these homogeneous regions can be defined using the analyst's knowledge of the area. Also in the second part of the SSC method, the analyst can interfere in the classification process by extending the number of runs for expansion of the homogeneous regions. He is also able to adjust the ratio between the spatial and the spectral influence, which can be helpful if little is known about the area to be classified.

In results as in figure 5 it can be seen that due to the expanding method for homogeneous regions, they have an increased influence in the classification process. In combination with line detection techniques, it should be possible to extract for example line forms to use as an input in the SSC classification process and in that way assigning the same influence to other topographic features in the image. That was however outside the scope of this study.

The results show that mixed pixels may cause spectral confusion and may then be assigned to the wrong class. The SSC method illustrates that it is possibly to apply alternative techniques for detecting and assigning mixed pixels. The homogeneous areas for example can be used as an information base for subpixel classification techniques such as spectral unmixing techniques (Adams et al, 1995; Van der Meer & De Jong., in press). In spectral unmixing techniques the spectral signature of a pixel is sub divided into the potential classes that contribute to the mixing of the spectral signature of a pixel. By using the SSC classification, assumptions on the endmembers of the pixel to be investigated can be made.

## 5 CONCLUSIONS

Results of the SSC (Spatial and Spectral Classification) method show that image classification of spectroscopical images can significantly improve by capturing spatial information in the classification procedure. The SSC method accounts for spatial information in an image in two ways. Homogeneous regions are extracted using the spectral profile plot. This information is used to classify the homogeneous parts of the imaging spectroscopy image. Next, as the location of homogeneous areas is known, this information is then used for the classification of the remaining pixels. Results of comparative tests with conventional classification methods yield promising results and illustrates the potential of this new proposed method.

## ACKNOWLEDGMENTS

Mr A.Lucieer and ms E.Koster are kindly acknowledged for providing the field reference dataset for validating the SSC method.

## REFERENCES

- Adams J.B., Sabol D.E., Kapos V., Almeida Filho R., Roberts D.A., Smith M.O., Gillespie A.R., 1995, 'Classification of multi-spectral images based on fractions of endmembers: Applications to land-cover changes in the Brazilian Amazon.' *Remote sensing of Environment*, 52, pp.137-154.
- Aplin P., Atkinson P.M., Curran P.J., 1999, 'Fine spatial resolution simulated satellite sensor imagery for land cover mapping in the United Kingdom'. *Remote sensing of Environment*, 68, pp. 206-216.
- Bryant J., 1979, 'On the clustering of multidimensional pictorial data'. *Pattern recognition*, 11, pp. 115-125.
- Burrough P.A., MacDonnell R.A., 1998, *Principles of Geographical Information Systems*. Oxford: Oxford University Press, 333pp.
- Crósta A.P., Sabine C., Taranik J.V., 1996,, 'A comparison of image processing methods for alteration mapping'. *Proceedings of the sixth Annual JPL Airborne Earth Science workshop*, Pasadena, California.
- De Jong S.M., Burrough P.A., 1995, 'A fractal approach to the classification of Mediterranean vegetation types in remotely sensed images'. *Photogrammetric Engineering & Remote Sensing* 61, no.8, pp.1041-1053.

De Jong S.M., Sommer S., Lacaze B., Scholte K., Meer F. van der., 1998, 'The DAIS La Peyne experiment: Using airborne imaging spectrometry for land degradation survey and modelling'. *Proceedings 18<sup>th</sup> EARSeL Symposium on operational Remote Sensing for sustainable development*, Enschede, The Netherlands.

DeMon-II, 2000: *An integrated approach to assess and monitor desertification processes in the Mediterranean basin*. Utrecht University, Utrecht, The Netherlands. <http://www.geog.uu.nl/dais/> (23 March 2000)

Goetz A.F.H., Vane G., Solomon J.E., Rock B.N., 1985, 'Imaging spectrometry for earth remote sensing'. *Science* 228, pp.1147-1153.

Hornstra T.J., Lemmens M.J.P.M., Wright G.L. 1999, 'Incorporating intra-pixel reflectance variability in the multispectral classification process of high-resolution satellite imagery of urbanised areas'. *Cartography*, 28, vol. 2. pp 1-9.

Institut für Optoelektronik, 2000, *The Digital Airborne Imaging Spectrometer DAIS 7915*. DLR, German Aerospace Center, Linder Höhe. <http://www.op.dlr.de/dais/dais-scr.htm> (17 March 2000)

Janssen L.F., Molenaar M., 1995, 'Terrain objects, their dynamics and their monitoring by the integration of GIS and remote sensing'. *IEEE transactions on geoscience and remote sensing*, 33, no. 3, pp. 749-758.

Kettig R.L., Landgrebe D.A., 1976, 'Classification of multispectral image data by extraction and classification of homogeneous objects'. *IEEE transactions on geoscience electronics*, ge-14, pp. 19- 26.

Kruse F.A., Lefkoff A.B., Boardman J.W., Heidebrecht K.B., Shapiro A.T., Barloon P.J., Goetz A.F.H., 1993, 'The spectral image processing system (SIPS) - Interactive visualization and analysis of imaging spectrometer data'. *Remote sensing of environment*, 44, pp. 145-163.

McCormick N., 1996, 'Automated forest stand mapping by spatial analysis of satellite imagery', *Proceedings international workshop Application of remote sensing in European forest monitoring*, Vienna, Austria 14-16 October 1996.

Ryherd S., Woodcock C., 1996, 'Combining spectral and texture data in the segmentation of remotely sensed images'. *Photogrammetric Engineering & Remote Sensing*, 62, p.181-194.

St-Onge B., 1999, 'Topographic effects on the texture of high-resolution forest-stand images measured by the semivariogram'. *Photogrammetric Engineering and Remote Sensing*, 65, pp. 923-935.

Van der Meer F., Bakker W., 1997, Cross correlogram spectral matching: Application to surface mineralogical mapping by using AVIRIS data from Cuprite, Nevada. *Remote sensing of Environment*, 61, pp. 371-382.

Van der Meer F., De Jong S.M., Improving the results of spectral unmixing of Landsat Thematic mapper imagery by enhancing the orthogonality of end-members. *Int. Journal of Remote Sensing*, in press.